68th International Astronautical Congress (IAC), Adelaide, Australia, 25-29 September 2017.

IAC-17-C2.7.9

A trade-off study on the mechanical support structure of the MASCOT-2 small body lander package

Michael Lange[a]*, Christian Hühne[a], Caroline Lange[b], Olaf Mierheim[a]

[a] *Institute of Composites Structures and Adaptive Systems, DLR – German Aerospace Center , Lilienthalplatz 7, 38100 Braunschweig, Germany*, m.lange@dlr.de
[b] *Institute of Space Systems, DLR – German Aerospace Center , Robert-Hooke-Strasse 7, 28359 Bremen, Germany, Caroline.Lange@dlr.de*, caroline.lange@dlr.de
* Corresponding Author

Abstract

The Mobile Asteroid surface SCOuT (MASCOT) is a 11 kg small body lander package developed under DLR lead for the Japanese space probe Hayabusa2. Based on MASCOT a modified MASCOT-2 lander package was studied for the AIM (Asteroid Impact Mission) mission study. The objective of the study was to develop a lander package, which maximizes heritage and reuse from the MASCOT predecessor. Thus the landing module's framework structure retained the MASCOT design variant, being up-scaled by approx. 20% (MASCOT-2: 330mm x 300mm x 210mm, 13 kg). In contrast, the interface structure called Mechanical and Electrical Support Structure (MESS) experienced a more significant re-design, due to the need of interface simplification and the peculiarities of the lander deployment for AIM mission and the Didymos system. This paper introduces three possible design variants for the MESS, which are later narrowed down to two and presented in greater detail: a CFRP-honeycomb sandwich plate with additional unidirectional stiffening plies and an X-shaped solid CFRP hat beam structure. Both variants are much simplified compared to the MASCOT support structure, but retain the overall mounting variant. This conceptual discussion is followed by a detailed structural analysis of both mechanical support structures. Provided by a set of mechanical loads and stiffness requirements, the sandwich and beam interface structures are separately simulated in a finite element model, consisting of shell and beam elements, respectively. The attached landing module is modelled with both, shell and beam elements, allowing a coupled structural analysis of the system. By varying geometrical and material parameters in the structural MESS models, a trade-off between the resulting minimal masses, the stiffness and the strength requirements is performed. Specifically considering also development risks it is concluded that the sandwich design variant shows an overall better performance.
Keywords: MASCOT, AIM, interface structure, CFRP, finite element simulation

Acronyms/Abbreviations

AIDA	Asteroid Impact & Deflection Assessment
AIM	Asteroid Impact Mission
APL	Johns Hopkins Applied Physics Laboratory
CFRP	Carbon Fibre Reinforced Plastic
DART	Double Asteroid Redirection Test
DLR	German Aerospace Centre
ESA	European Space Agency
MASCOT	Mobile Asteroid surface SCOuT
MESS	Mechanical and Electrical Support Structure
NASA	National Aeronautics and Space Administration
S/C	Spacecraft

1. Introduction

Near-Earth objects' exploration is in the focus of various stakeholders, ranging from planetary defence over science and human exploration to resource utilization. Especially after the Chelyabinsk meteor airburst in February 2013 public awareness was raised, leading to an increased discussion of asteroid threat and planetary defence [1]. In the same context and based on a simplified scenario of the European Space Agency's (ESA) "Don Quijote" concept, Johns Hopkins Applied Physics Laboratory (APL) has identified a joint mission of opportunity named Asteroid Impact & Deflection Assessment, AIDA [2–4]. It consists of two independent mission concepts studied by ESA and NASA/APL, the Double Asteroid Redirection Test (DART) and Asteroid Impact Mission (AIM), respectively. Both target the binary Near-Earth asteroid system 65803 (1996 GT) Didymos. The smaller member of this system, "Didymoon", is supposed to be impacted by the DART spacecraft (S/C) in October 2022. At the same time, the AIM S/C will have characterized the binary asteroid system and monitor the DART impact. Subsequently it determines the momentum transfer on Didymoon. In order to support the characterization phase and the impact monitoring, the German Aerospace Centre (DLR) studied the MASCOT-2 (Mobile Asteroid surface SCOuT) lander package, a successor of the MASCOT lander. However, as AIM did not receive full funding on the ESA Ministerial Council 2016, MASCOT-2 specific developments are discontinued at the time of writing. Yet, the MASCOT system is

considered a potential autonomous, adaptable and mobile instruments carrier for other future small body exploration missions. Currently the first MASCOT is on its cruise onboard the Japanese Hayabusa2 space probe [5,6] towards the asteroid 162173 Ryugu (1999 JU_3). Once deployed and landed on Ryugu, MASCOT will provide ground truth for the instruments onboard the main S/C, in-situ reference measurements and perform stand-alone experiments. The MASCOT structure consists of two main components, the actual landing module and a mechanical support structure (MESS), connecting the lander to the Hayabusa2 S/C. Both structural components are based on a highly stiff and lightweight composite framework structure with a minimal first system eigenfrequency of 120 Hz. Its total size is 28 cm × 29 cm × 21 cm and the total mass is of ~10 kg [7].

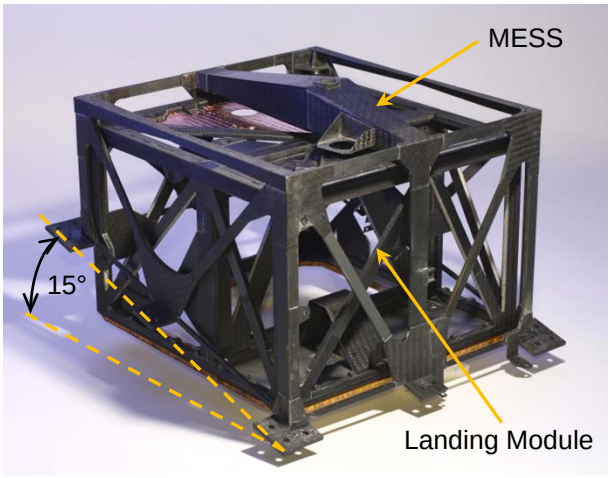

Figure 1. MASCOT landing module and mechanical support structure (MESS).

1.1 Outline

Based on its predecessor's design a modified MASCOT-2 lander package was studied for the AIM mission study. Its main objective was to develop a lander package that maximizes heritage and reuse from MASCOT [8,9]. That is, the landing module's framework structure retained the MASCOT design concept, being up-scaled by approx. 20%. In contrast, the MESS experienced a re-design due to the need of interface simplification and the peculiarities of the lander deployment for the AIM scenario.

Focussing in this paper on the mechanical support structures' re-design, at first the initial system and structural requirements are summarized in section 2. Section 3 introduces to the MASCOT-2 design including three possible MESS variants, which are subsequently narrowed down to two and presented in greater detail. In section 4 the preceding conceptual discussions is followed by a detailed structural analysis of the two favoured mechanical support structures. Provided by a set of mechanical loads and stiffness requirements, the sandwich and beam interface structures are separately simulated in a finite element model, consisting of shell and beam elements, respectively. By varying geometrical and material parameters in the structural models, a trade-off between the resulting minimal masses, the stiffness and the strength requirements is performed.

Finally, section 5 concludes and summarizes the findings of the MASCOT-2 trade-off study for the AIM mission study.

2. System and structural requirements

Based on the experiences with MASCOT and Hayabusa2, the AIM study requirements were defined and updated to fit the new scenario. Listed in the following is an extract of system requirements relevant for the structural design of the MASCOT-2 MESS [10]:

SYS-1: The MASCOT-2 system shall be compatible with a Soyuz 2-1b Fregat launcher and its defined launch environment to be launched from Kourou.

SYS-2: The maximum mass of the MASCOT-2 system, excluding Bistatic radar orbiter parts, shall not exceed 13 kg including maturity margins.

SYS-3: The maximum MASCOT-2 system volume (stowed configuration) (…) shall not exceed (301 [X-width] x 301 [Y-depth] x 360 [Z-height]) mm³ (TBC).

SYS-4: The MESS shall remain attached to main- S/C after the lander deployment.

SYS-5: The MESS shall not disturb the main-S/C operations after lander deployment.

SYS-6: The MESS shall be aligned with an accuracy of 1° in parallel to the side panel of the AIM S/C from which it is deployed.

SYS-7: MASCOT-2 system shall be designed to provide the required performance when subjected to all mechanical, static and dynamic loads encountered during its entire design lifetime (…).

Additionally, specific structural requirements are defined, based on best knowledge according to the information available on the launcher and AIM mother S/C at the point in time when the study was performed:

STR-1: The total structural mass of the landing module plus MESS shall be below 2.65 kg.

STR-2: The first global eigenfrequency of the MASCOT-2 system should be higher than 100 Hz.

STR-3: The design limit load should be 13.8G in X-, Y- and Y-direction.

STR-1 is based on the assumption that the structural mass of MASCOT-2 will grow by 20% linearly with its volume. Main reasons for the growth are an additional mobility mechanism and the exchange of the *MicrOmega* instrument (MASCOT) with an AIM-specific low-frequency radar. STR-2 and STR-3 are defined by engineering judgment as no detailed information on the mother S/C was available at that point in time. Hence, the design limit load is derived from the Ariane 5 Structure for Auxiliary Payload manual for a micro payload [11]. Additional factors of safety take into account the early project phase, model uncertainties and the qualification margin as listed in Table 1. This results in total in a design limit load of: 8G * 1.725 = 13.8G.

Table 1. Factors of Safety [12].

Type of uncertainty	Factor of safety
Project Factor	1.15
Model Factor	1.2
Qualification Factor	1.25
Total factor	**1.725**

3. MASCOT-2 structural design

A major difference between MASCOT and MASCOT-2 would be that the anterior one was designed for a basically existing S/C, Hayabusa2, which was already a successor of the first Japanese asteroid sample return mission Hayabusa. In case of AIM, the lander and the mother S/C would be developed at the same time with parallel development phases. Additionally, although not an actual requirement, it was the goal to reuse as much as possible of the MASCOT design in order to reduce the development costs. Therefore the MASCOT landing module's framework structure is retained and up-scaled by approximately 20%. Minor modifications allow the integration of the low-frequency radar electronic box and a re-designed common electronic box, which will house two mobility mechanisms instead of one as for MASCOT. The mechanical connection between the landing module and the MESS structure is the same as applied for MASCOT. It is realised by a central bolt connecting the interface structure with a non-explosive actuator in the landing module's central framework wall (cf Figure 8 and Figure 8). The bolt pulls four bearing points, which are located in the landing module's bottom side corners, into their counterparts on the interface structure. For more details refer to [5,7].

On the other hand the MESS structure is simplified for the AIM scenario. For Hayabusa2, its design was constrained by two requirements imposed by the solar array panel (SAP), which is in the stored configuration in front of the MASCOT lander. In order to avoid collisions at lander deployment, the MESS had to be built with a negative inclination of 15° to the -Y–panel of Hayabusa2. Further the lander package was not allowed to protrude more than 80mm out of Hayabusa2 -Y–Plane (see Figure 2). The complex design however lead to further risks on lander deployment side by producing potential obstacles for a smooth separation of the lander out of its pocket. The created pocket in the Hayabusa2 structure also resulted in further requirements regarding thermal isolation posed upon the MESS design.

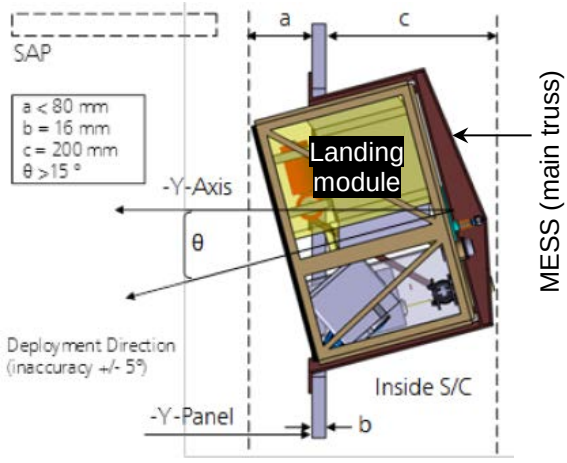

Figure 2. Inclined MASCOT landing module (beige) in MESS support structure (brown) mounted to the Hayabusa2 -Y–plane. In dashed lines the position of the stored and deployed solar array panel (SAP), respectively.

As the described design constraints do not apply for AIM, a re-design of the MESS in correspondence with the AIM S/C allows major simplifications and risk mitigation. Figure 3 depicts two principal design options as a modification of the MASCOT MESS structure. Option 1 retains the MASCOT MESS design, but has no inclination. As a consequence the landing module has to pass less MESS structure (z = TBD mm), reducing the probability of hitting it during separation. Also the MESS build is much simplified. The most extreme case ($z \approx 0$ mm) retains only the structural main part of the MASCOT MESS, i.e. its main truss/ bending beam, while additional extensions and a load redirecting framework structure are no longer required. Further the inside volume of the mother S/C is enlarged while the surface to be thermally shielded after the landing module's separation is minimized. Option 2 (in two variants) is a mostly new design, but based on very simple and plane structures. Instead of one central truss as in the MASCOT case, the MASCOT-2 MESS has an X-shaped support platform with two intersecting bending beams (Opt. 2, variant M-1; cf Figure 4) or an

X-stiffened sandwich plate (Opt. 2, variant M-2; cf Figure 5). Both alternatives are mounted outside and on top of an AIM S/C's panel.

Eventually, option 2 is preferred, because of the following reasons:

2. An inclination is not required for the AIM S/C design.
3. The MESS design and manufacturing is much simplified.
4. A cut-out in the mother S/C panel is avoided.
5. Option 2 promises a higher stiffness/mass ratio

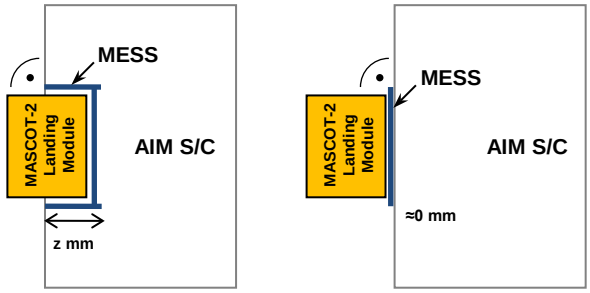

(1) (2)

Figure 3. Alternative MESS design concepts. Opt. (1): Recessed in mother S/C panel, w/o inclination. Opt. (2): Flat-mounted on an outer panel of the AIM S/C.

4. MESS trade-off study

After discarding the recessed MESS configuration (option (1)), the following trade-off study considers only the two flat-mounted variants introduced as option 2. Both provide a dedicated flat-mounted interface to the lander. Hereinafter, the two variants are distinguished in as:

M-1: X-shaped bending beam structure
M-2: CFRP-honeycomb sandwich plate with additional unidirectional (UD) X-stiffening CFRP plies

Figure 4 illustrates the principal layout of variant M-1. It consists of two crossing bending beams with a cross section, that could be either of "I"[(1)], "Omega"[(2)] or "Hat"[(3)] shape. In terms of manufacturing and interface implementation the hat-shaped cross section offers several benefits and is therefore chosen as baseline beam profile. A central bolt with a non-explosive actuator is pulling the four bearing points, located in the landing module's corners, into the beam's corresponding counterparts. Both bearing points have the same design as for MASCOT. The X-shaped interface structure itself is mounted at the four bending beams' tips to a panel of the AIM S/C (cf Figure 8). Variant M-2 is proposed as a CFRP-honeycomb sandwich plate with an additional unidirectional X-stiffening as sketched in Figure 5. The unidirectional stiffening is applied on both face sheets of the MESS sandwich plate supporting the panel under bending loads introduced by the non-explosive actuator. The positions of the actuator and the bearing points are the same as for variant M-1. Also the connection between MESS and the AIM S/C panel is comparable to variant M-1 (cf Figure 8).

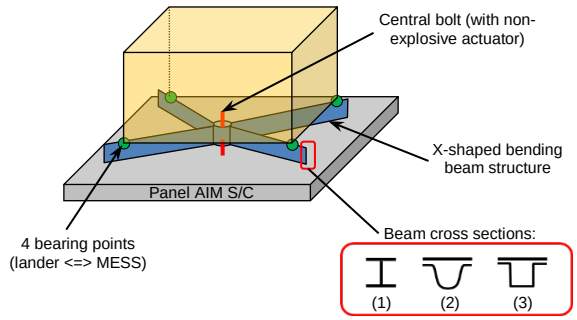

Figure 4: Variant M-1, X-shaped bending beams.

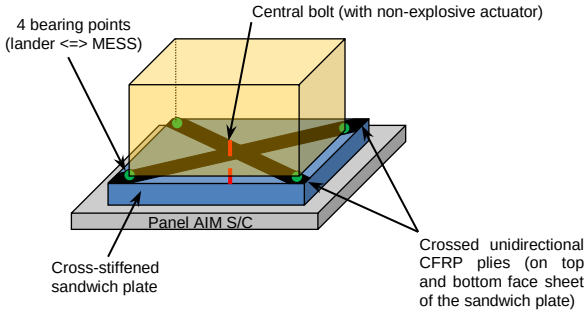

Figure 5. Variant M-2, cross-stiffened sandwich plate.

5.1 Mechanical analysis

The mechanical analysis of the two MESS variants is subdivided in three parts: an introduction into the PATRAN/NASTRAN finite element model, followed by a numerical stiffness analysis and subsequently a numerical strength analysis of both MESS variants M-1 and M-2.

5.1.1 Finite Element Model

The MASCOT-2 finite element model consists of two parts, a landing module model and a MESS model. This allows to include two separate MESS models one by one in the simulation and to run a jointed simulation with exactly the same landing module model. Same as for MASCOT, the finite element model is based on 1-D elements (beams of MESS M-1 structure) and 2-D elements for the structural parts of the landing module and the MESS (cf Figure 8). The 1-D elements are of type BAR2 and the 2-D elements of type QUAD4.

To differentiate between each design variation Figure 7 introduces a naming convention for the

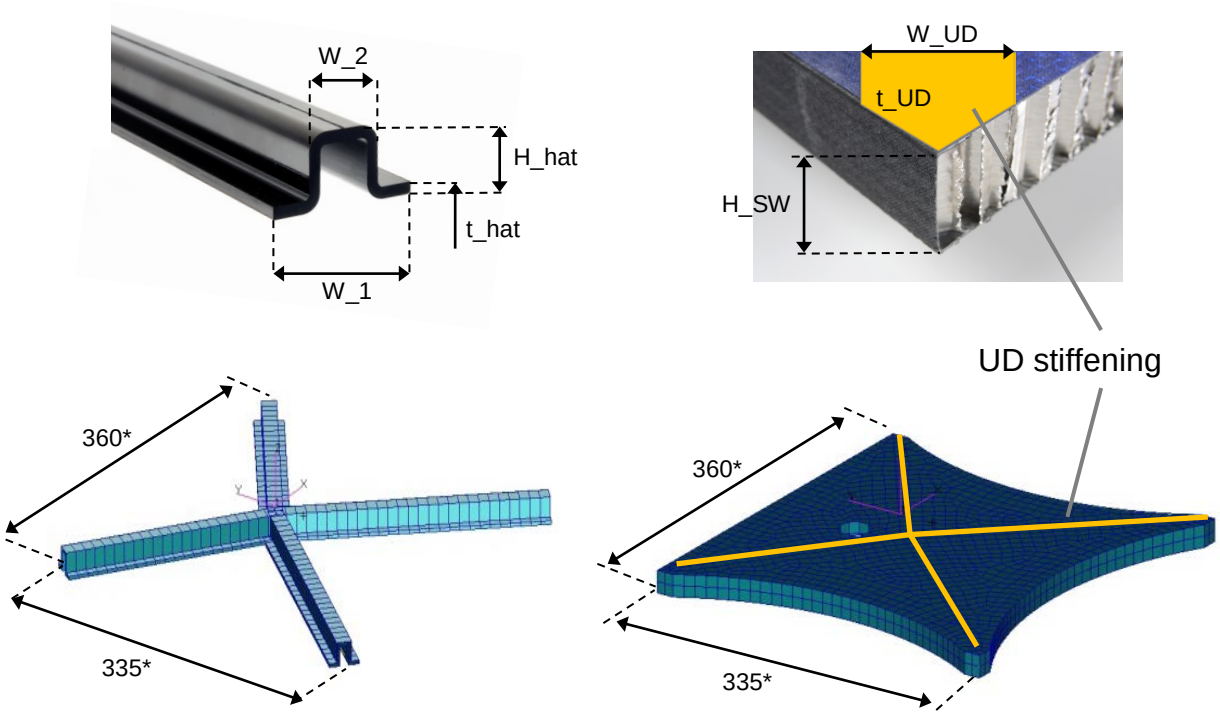

Figure 6. Naming convention and dimensions of the MESS design variations (M-1, left and M-2, right).

* The distances in [mm] are given between the I/F points as simulated in the FE model.

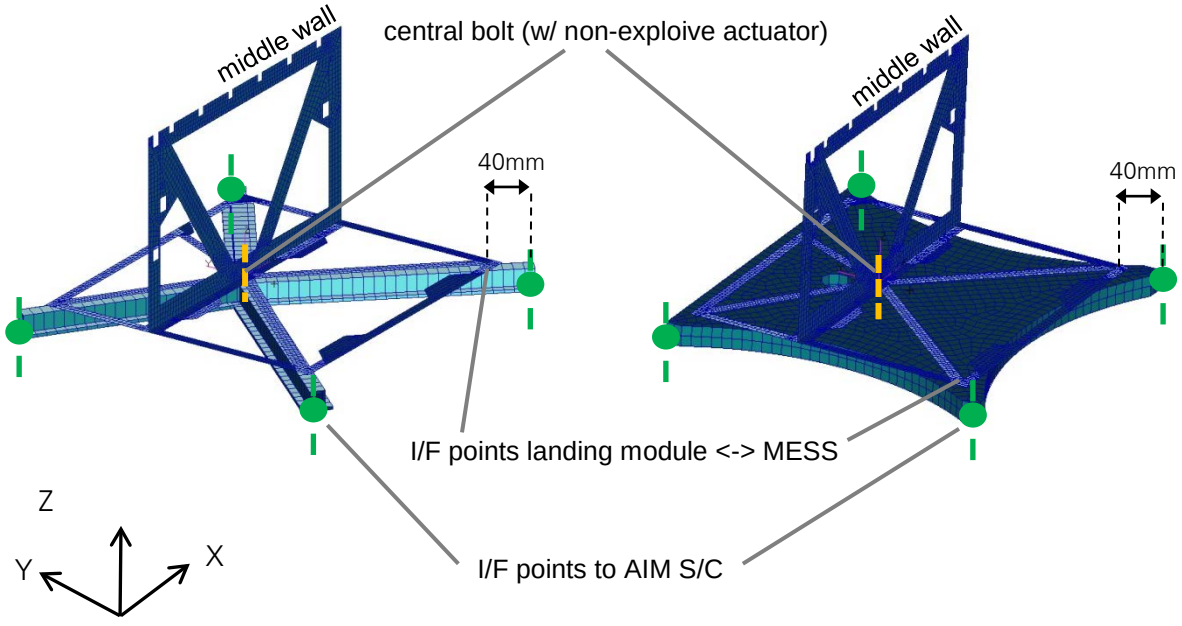

Figure 7. MESS M-1 (left) and M-2 (right) as implemented into the FE model with the landing module's bottom plate, middle wall and interface points. For visual reasons the 1-D and 2-D MESS finite elements are extruded to 3-D.

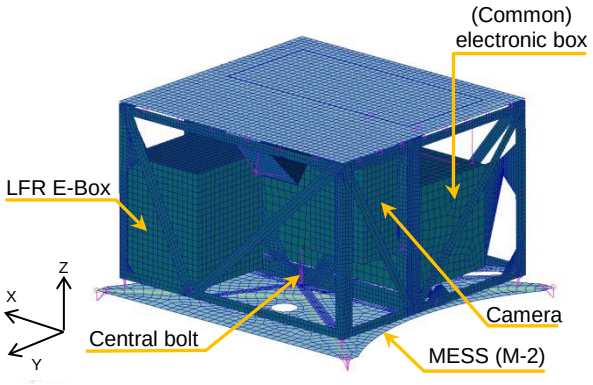

Figure 8. Finite element model of the MASCOT-2 landing module jointed MESS M-1.

following variable parameters:

- The total height of the sandwich and the hat beam structure, H_hat and H_SW, respectively.
- The laminate's thickness t_hat of the hat beam structure.

For example, HAT: 20-2 means a hat beam profile with a total height of H_hat = 20 mm and a laminate thickness of t_hat = 2 mm. Similar SW: 10+1 refers to a sandwich plate with a thickness of H_SW = 10 mm and an additional UD-ply stiffening on top and bottom face sheet of t_UD = 0.5 mm each. The other dimensions are set to W_1 = 30.0 mm, W_2 = 15.0 mm, while the interface (I/F) points to the AIM S/C have a distance of 335 mm in Y-direction and 360 mm in X-direction, respectively. Although potentially not compliant with SYS-3 (TBC) requirement, it is decided to maintain this dimension. The geometric position of the central bolt (cf Figure 8) is kept fixed, too.

To simulate the UD-stiffening on the sandwich plate an I-Beam (CBAR element) is created that has a web of 0.01 mm thickness and a height of H_SW (cf Figure 9). Hence, the web's contribution to the sandwich's bending stiffness can be neglected and the actual UD-plies are simulated with a thickness of t_UD = 0.5 mm and a width of W_UD = 20.0 mm.

Figure 8 shows how both design variations are implemented into the finite element model. For a better visual presentation all BAR and QUAD elements (except the I-Beam) are extruded to 3-D elements. The four connections between the landing module and the MESS as well as the four interfaces between the MESS and the AIM mother S/C are simulated with RBE2 elements. In case of the former interface, all degrees of freedom are constrained, while for the latter one the angular displacements are unconstrained. The distance between the interface I/F points (landing module to MESS and MESS to AIM S/C) in the X-Y-plane is ≈ 40 mm. The central bolt is simulated by two opposing forces. These pull on both structures, simulating a pretension in the bolt, which has to be sufficiently high in order to realize permanent contact between the bearing points of the landing module and the MESS under all loading conditions.

The total mass of the landing module, which is implemented in the finite element model, is 8.54 kg. This includes 1.08 kg primary structures and a common electronic box of 0.8 kg. The actual lander package will be heavier due to the fact that the study model does not consider harness, solar cells eventually distributed evenly on the outer lander surfaces and a calibration target.

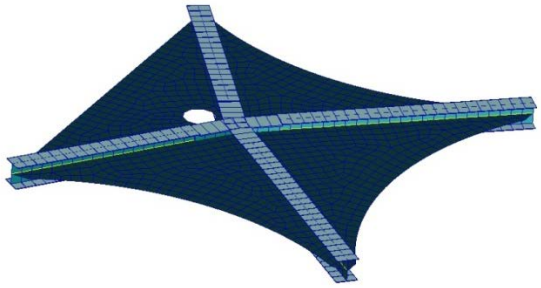

Figure 9. Modelling of the UD-stiffening. For visualisation the BAR elements are extruded.

5.1.2 Material properties

The laminate and sandwich plate of MESS M-1 and M-2, respectively, are simulated with the materials listed in Table 2. Metallic parts, such as flanges, consist of aluminium alloy EN AW-7075.

The material properties of the fibre composites, aluminium honeycomb sheets and aluminium are listed in Table 3. While the M55J/EX-1515 is an UD prepreg system used for the sandwich plate's X-stiffening and the X-beams, M40J/L160-H163 is a 0°/90° fabric. It is applied in a hand lay-up process for the face sheets of the sandwich. Its core is made from aluminium honeycomb sheets PAMG-XR1-3.0-3/8-002-P-5052.

Table 2. MESS M-1 and M-2 constituents.

Design variant	Material
MESS M-1	M40J/MTM46
MESS M-2	M40J/L160-H163 PAMG-XR1-3.0-3/8-002-P-5052 M55J/EX-1515

5.1.3 Stiffness analysis

In order to compare the effect of geometrical changes on the first global eigenfrequency for the two MESS variants a stiffness analysis is performed. For that both MESS variants are simulated in a coupled

Table 3. Material properties.

Material Parameter	M55J/ EX-1515*	M40J fabric/ L160- H163**	PAMG-XR1- 3.1-3/8-002- P-5052	Aluminium (7075)
E_{11} [N/mm²]	300000	95000	5	72000
E_{22} [N/mm²]	6000	95000	5	-
E_{33} [N/mm²]	-	-	480	-
Nu_{12} [-]	0.23	0.4	0.25	
Nu_{23} [-]	-	-	0.15	0.33
Nu_{13} [-]	-	-	0.25	
G_{12} [N/mm²]	4000	37600	2.5	
G_{23} [N/mm²]	4000	3380	145	27000
G_{13} [N/mm²]	4000	3380	295	
ρ [g/cm³]	1.54	1.45	0.05	2.7
X [με]	3000	4000	-	50000
Y [με]	3000	4000	-	50000
$X_{tension}$ [N/mm²]	-	-	-	-
$X_{compr.}$ [N/mm²]	-	-	1.79	-

* f-vol.=55%** f-vol.=50%

system with the landing module and also separately. The simulation of the M-1 variant (X-shaped bending beams with hat cross-section) is based on two heights and thicknesses of the hat profile. For the M-2 variant (cross-stiffened sandwich plate) three different sandwich cores, with 10 mm, 15 mm and 20 mm are simulated. The results of the analysis are listed in Table 4.

Three major observations, which can be derived from the obtained results, shall be highlighted in the following:

1. In addition to the global eigenfrequencies listed in Table 4, two local eigenfrequency are found in the coupled simulations at ≈ 127 Hz and ≈ 143 Hz. They are related to the camera and the LFR E-Box, respectively, and therefore independent from the MESS structure. The first global eigenfrequency does not vary significantly with the structural changes on the MESS variants and is found for each variant in the range of ≈ 170-185 Hz. Though, while the coupled systems corresponding eigenmode is a rotation in the XY-plane for variant M-1 it is a rotation in the XZ-plane for variant M-2.
2. The first eigenfrequency in the separate simulation shows quite different results for the MESS variants. For variant M-1 there is a significant difference between a 15 mm and 20 mm high hat profile. The influence of the profile's thickness t_hat on the eigenfrequency can be neglected, while the mass increases significantly. This seems to be also the reason for the slightly lower first eigenfrequency, when comparing variant HAT: 15-2 to HAT: 15-3 and HAT: 20-2 to HAT: 20-3, respectively.

   Though, variant M-1 (t_hat = 2 mm) offers the stiffer and lighter structural design for a comparable height of the MESS (H_hat and H_SW). This does not change when the flanges are included in the mass calculation either. On the other hand, variant M-2 allows increasing the stiffness with almost no increase of the mass. This is possible, because only the honeycomb core with its very low density has to be changed in height, while the CFRP face sheets remain unchanged.
3. STR-2 (1. EF > 100 Hz) is distinctly fulfilled by each type of both variants.

   However, in order to integrate the separation mechanism in the MESS, the variants with a thickness of 20 mm are preferred.

Table 4. Results of the coupled stiffness analysis for MESS variant M-1 and M-2.

Variant	Type	Mass FEM [g]	Mass flanges* [g]	1. EF [Hz] (global)	1. EF [Hz] (MESS)
M-1	HAT: 15-2	170	100	177	676
	HAT: 15-3	245	100	183	652
	HAT: 20-2	200	140	168	833
	HAT: 20-3	290	140	177	813
M-2	SW: 10+1	207	160	174	485
	SW: 15+1	207	200	181	618
	SW: 20+1	220	200	185	720

* estimated

5.1.4 Strength analysis

The strength analysis applies a static load of 13.8G in X-, Y- and Z-direction separately to the MASCOT-2 finite element model. As stated in subsection 5.1.3 the 20 mm MESS configurations are preferred. Therefore, only the lighter M-1 variant, HAT: 20-2, and the corresponding M-2 variant, SW: 20+1, are compared to each other. Both have a similar mass (when flanges are excluded) and geometry in terms of height. Also the resulting first (global) eigenfrequencies in the coupled simulation are comparable. To evaluate the structures strength the allowable strain is set to 3000με and 4000με for the M55J prepreg system and M40J fabric, respectively.

However, in order to indicate a ply failure due to excessive strain the strains are plotted in the results between ±3000 με only. This allows a better comparability of the fringe plots amongst each other. Further the load case (LC) descriptions in the fringe plots refer to coordinate system "0" (CS-0). This is depicted in the fringe plot's lower left corner.

Exemplarily for the MESS M-1 variant, Figure 10

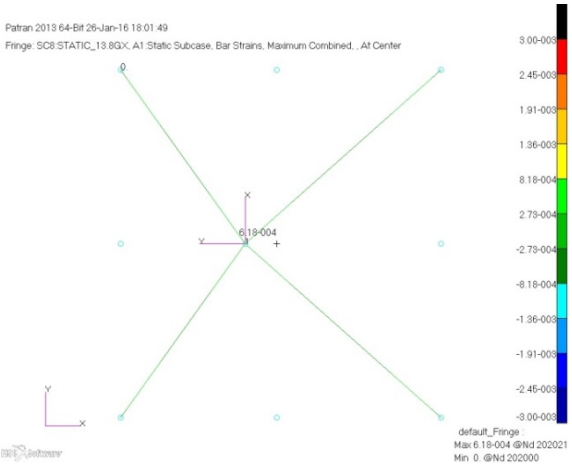

Figure 10. LC: 13.8G in X-direction (CS-0); Result: max. strain (combined).

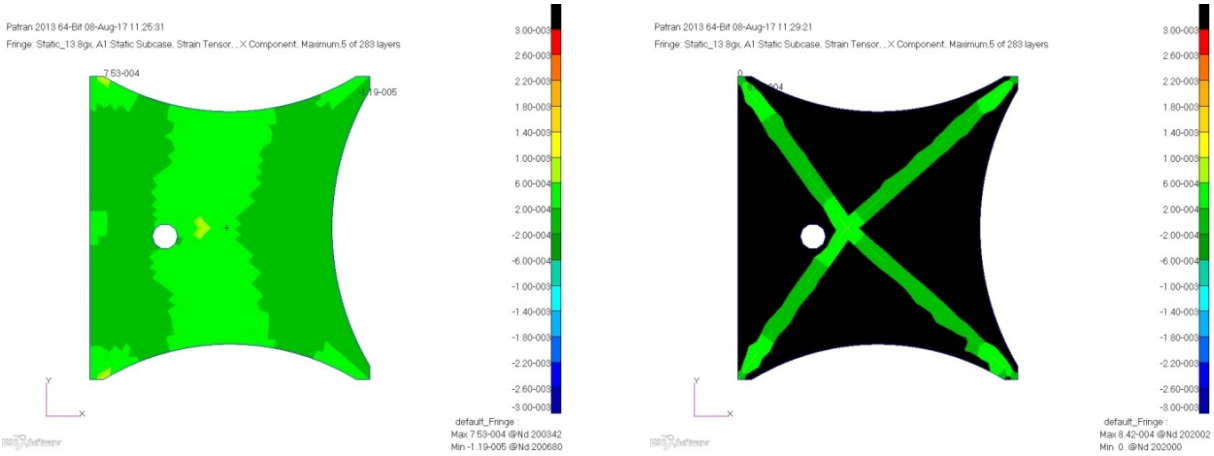

Figure 11. LC: 13.8G in X-direction (CS-0); Result: X-strain. Honeycomb + Face Sheets (left), UD-stiffeners (right).

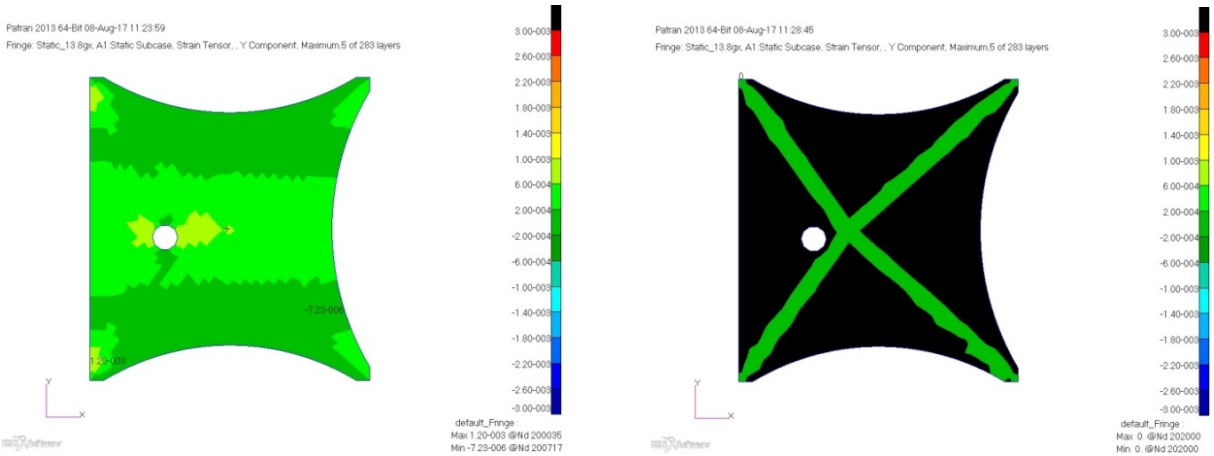

Figure 12. LC: 13.8G in X-direction (CS-0); Result: Y-strain. Honeycomb + Face Sheets (left), UD-stiffeners (right).

shows the resulting strains due to a static load of 13.8G in X-direction. As the MESS M-1 variant is simulated with beam elements, the presented results show the maximum combined strain due to a bending and normal (axial) load contribution. The maximum strain occurs in the crossing of the four struts where the central bolt is located. The beam's tip points experience no strain in the simulation as they are constrained. Further the overall strain distribution is basically symmetric with respect to the XZ- and YZ-planes. The results for a loading in Y- and Z-direction are comparably low and similarly distributed. Hence for no load case the maximum allowable strain is exceeded.

In comparison to the hat beam results the MESS M-2 sandwich plate's analysis (Figure 11 and Figure 12) is primarily subdivided in the results for the "actual" sandwich and the additional UD-stiffeners applied at the top and bottom face sheet. Again the strains are plotted between ±3000με, in order to indicate a ply failure due to excessive strain immediately. The direction of the applied load is always applied with respect to the coordinate system "0" (CS-0), depicted in the plots lower left corner.

The X-strain results for the honeycomb+facesheet in Figure 11 (left) show the highest strains in the sandwich plate's "wings" and in the centre. With a maximum of ≈ +750με this is well below the allowable strain. As to be expected, also the corresponding X-strains in the UD-stiffeners (Figure 11, right) are quite low. The corresponding distribution is comparable to the results of the hat beam structure, which is due to the fact that both are simulated as bar elements having the same boundary conditions. Consequently, the simulation as bar element is also the reason for a zero—id est not calculated—Y-strain distribution in Figure 12, right. The Y-strain distribution for the honeycomb+facesheet shows basically the X-strain distribution, but mirrored on a 45°-axis, and a maximum strain of +1200με. The results for a Y- and Z-directional loading of the MESS M-2 variant are very similar and not shown for brevity.

In summary, for both MESS variants the maximal occurring strains are well below the maximum allowable strains. Further, the strain distributions are for each load case very similar. This indicates that the NEA bolt's load is dominating the stress/strain state and that it is basically independent of the applied load case (direction).

5. Conclusion

From section 4 it is concluded that both MESS variants potentially fulfil the mechanical requirements. Both can be designed with a sufficiently high stiffness and strength, while having a similar mass. The latter is based on the fact that the non-explosive separation system has to be integrated into the MESS structure as well. Therefore it is not favoured to design a MESS structure of less than 20 mm in height. Both, the M-1 and M-2 variant weigh (without flanges) in the HAT: 20-2 and SW: 20+1 configuration, respectively, approximately 200g. Including the estimated mass for flanges, the M-1 variant will be probably lighter and preferred. On the other hand, the low strains in the UD-stiffeners of MESS M-2 indicate that these may not be required and some mass savings might be possible.

Looking also into secondary mechanical and non-mechanical requirements further differentiation is possible. These additional requirements (a weighting is not introduced) are:

- Low costs
- Minimizing additional developments and development risks
- Manufacturing and handling

Especially the required developments for the M-1 design, such as joining the struts and flange integration, bare an additional risk. In contrast the M-2 design is a "standard" and cheap sandwich construction with insert-like flanges. Similarly the qualified separation mechanism can be almost completely re-used with small adaptions only. The MESS M-2 sandwich will accommodate the separation mechanism in the same way as the MASCOT MESS, whose main beam is a sandwich design as well. In terms of the requirements SYS-3, SYS-4 and SYS-5 it has advantages over the M-1 design, too. The M-2 variant allows accommodating a required calibration target for the MASCOT on-board instruments on the MESS sandwich plate instead of mounting it on an AIM panel separately. Further the M-2 variant by virtue of its closed sandwich panel plane offers plenty of space for handling operations during the integration to the AIM spacecraft, when it's mated with the landing module. A general drawback of both design variants is that the lander's complete volume (SYS-3) is added on the outer surface of the AIM S/C. This is of no further issue for the AIM S/C, but has to be taken into account when considering the M-1 or M-2 design variants for future mission studies. After all, considering also secondary and non-mechanical requirements, the MESS M-2 variant is identified as the favoured structural design in this trade-off study. The final evaluation is summarized in Table 5.

Table 5. Summary – MESS trade-off

	MESS M-1	MESS M-2
Design	Both make use of a bending beam principal such as MASCOT MESS	
Stiffness & Strength	1. EF is local (camera) and independent of studied MESS designs 1. Global EF ≈ 170-185 Hz No strength issues	
Mass (incl. inserts and flanges)	Comparable (for thinner designs M-1 is lighter) For the separations mechanism's accommodation "thicker" designs, such as SW: 20+1, M-2 variant is preferred	
CalTarget	Requires further structure or mounting on AIM S/C	Can be mounted on MESS
Development & Manufacturing	More difficult and requires additional development; breadboard required	Standard design, no further development required MASCOT separation mechanism can be mostly re-used
Handling	Handling more difficult when the landing module is mounted to MESS	Better handling when the landing module is mounted to MESS

References

[1] J.T. Grundmann, C. Lange, B. Dachwald, C.D. Grimm, Small Spacecraft in planetary defence related applications - capabilities, constraints, challenges, in: IEEE Aerospace Conference, 2015, Big Sky, MT, 2015.

[2] A. Galvez, I. Carnelli, M. Khan, W. Martens, P. Michel, S. Ulamec et al., Asteroid Investigation Mission: The European contribution to the AIDA EU-US cooperation, in: 24th International Symposium on Space Flight Dynamics, Laurel, Maryland, USA, 2014.

[3] A.F. Cheng, J. Atchison, B. Kantsiper, A.S. Rivkin, A. Stickle, C. Reed et al., Asteroid Impact and Deflection Assessment mission, Acta Astronautica 115 (2015) 262–269.

[4] A.F. Cheng, AIDA: Asteroid Impact & Deflection Assessment - A Joint ESA-NASA Mission, Phoenix, AZ, 2015.

[5] T.-M. Ho, V. Baturkin, C. Grimm, J.T. Grundmann, C. Hobbie, E. Ksenik et al., MASCOT: The Mobile Asteroid Surface Scout Onboard the Hayabusa2 Mission, Space Sci Rev (2016).

[6] S.-i. Watanabe, Y. Tsuda, M. Yoshikawa, S. Tanaka, T. Saiki, S. Nakazawa, Hayabusa2 Mission Overview, Space Sci Rev (2017).

[7] M. Lange, O. Mierheim, C. Hühne, MASCOT, in: Proc. of 13th European Conference on Spacecraft Structures, Materials & Environmental Testing, Braunschweig, Germany: Structures design and qualification of an "organic" mobile lander platform for low gravity bodies., 2014.

[8] European Space Agency, Asteroid Impact Mission: Lander, [June 27, 2017], http://www.esa.int/Our_Activities/Space_Engineering_Technology/Asteroid_Impact_Mission/Lander.

[9] C. Lange, J. Biele, S. Ulamec, C. Krause, B. Cozzoni, O. Küchemann et al., MASCOT2, in: Proceedings of 68th International Astronautical Congress, Adelaide, Australia: A small body lander to investigate the interior of 65803 Didymos' moon in the frame of AIDA/AIM, 2017.

[10] C. Lange, AIM/MASCOT-2: Mission description document (MDD), Internal use, 2015.

[11] Arianespace - Technical Support Department, A.S.A.P. 5 - Ariane 5 Structure for Auxiliary Payload(Issue 1, Rev. 0), Evry Cedex, France, 2000.

[12] ESA-ESTEC - Requirements & Standards Division, Space engineering - Structural factors of safety for spaceflight hardware. 1st ed.(ECSS-E-ST-32-10C), Noordwijk, The Netherlands, 2009.